

Towards Effective User Attribution for Latent Diffusion Models via Watermark-Informed Blending

Yongyang Pan¹, Xiaohong Liu^{1*}, Siqi Luo¹, Yi Xin², Xiao Guo³,
Xiaoming Liu³, Xionguo Min¹, Guangtao Zhai¹

¹ Shanghai Jiao Tong University, ²Nanjing University, ³Michigan State University

Abstract

Rapid advancements in multimodal large language models have enabled the creation of hyper-realistic images from textual descriptions. However, these advancements also raise significant concerns about unauthorized use, which hinders their broader distribution. Traditional watermarking methods often require complex integration or degrade image quality. To address these challenges, we introduce a novel framework Towards Effective user Atribution for latent diffusion models via Watermark-Informed Blending (TEAWIB). TEAWIB incorporates a unique ready-to-use configuration approach that allows seamless integration of user-specific watermarks into generative models. This approach ensures that each user can directly apply a pre-configured set of parameters to the model without altering the original model parameters or compromising image quality. Additionally, noise and augmentation operations are embedded at the pixel level to further secure and stabilize watermarked images. Extensive experiments validate the effectiveness of TEAWIB, showcasing the state-of-the-art performance in perceptual quality and attribution accuracy.

Introduction

The advent of text-to-image models has revolutionized the creation of photorealistic images by transforming descriptive text into visually accurate representations, significantly advancing the capabilities of image synthesis (Nichol et al. 2021; Saharia et al. 2022; Guo et al. 2023; Liu et al. 2022; Yang et al. 2024). Contemporary Latent Diffusion Models (LDMs), including Stable Diffusion (Rombach et al. 2022) and DALL-E 2 (Ramesh et al. 2022), exhibit an impressive capacity to generate a wide range of novel images across diverse scenes and contents. While these advancements represent a substantial leap in AI-Generated Content (AIGC), they simultaneously raise concerns about the potential misuse of these models (Brundage et al. 2018).

Recent advances have significantly enhanced watermark embedding techniques in images (Zhu et al. 2018; Luo et al. 2020; Kishore et al. 2022; Fu et al. 2024; Wu et al. 2023). However, these methods are typically applied in a post-generation manner, making the watermarks vulnerable to manipulation, especially when models like Stable Diffusion (SD) (Rombach et al. 2022) are leaked or open-sourced. In

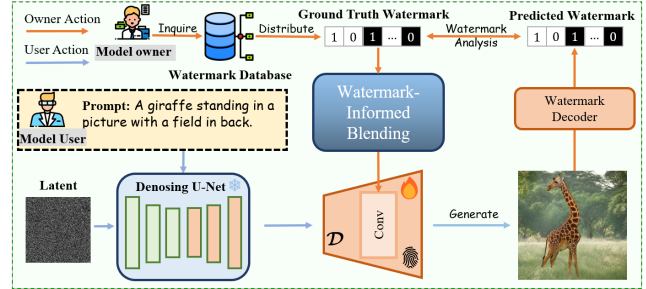


Figure 1: **Workflow of TEAWIB.** During inference, the finetuned model (*i.e.*, \mathcal{D}) is employed by the model user to generate images embedded with an invisible watermark. The model owner can then utilize the watermark decoder to identify watermarks within questionable images and trace their origins back to the respective model users.

these cases, a simple code modification can bypass the watermarking process. To address this vulnerability, the integration of watermark generation during the image creation process has emerged as a recent trend. For instance, Stable Signature (Fernandez et al. 2023) has developed an ad-hoc watermarking method that fine-tunes the decoder with a pre-defined watermark. Additionally, WOUAF (Kim et al. 2024) advances this approach by modifying decoder parameters during the image generation phase, thereby embedding watermarks more securely and supporting scalable watermarking.

Despite these advancements, integrated watermarking methods currently face two limitations. First, Stable Signature (Fernandez et al. 2023) requires retraining the model with each watermark update and only supports a single designated watermark, leading to training costs that scale linearly with the number of users. Second, methods like WOUAF, which modulate model parameters, can degrade image quality and increase vulnerability to post-processing attacks. Additionally, such methods require modifications to the base model parameters, further compromising the quality of the generated images.

To address these challenges, we introduce TEAWIB, a novel framework that adopts a proposed watermark-informed blending strategy, which comprises two compo-

*Corresponding author (email: xiaohongliu@sjtu.edu.cn).

nents: Dynamic Watermark Blending (DWB) and Image Quality Preservation (IQP). The DWB module includes watermark-specific weights, enabling the model to support scalable watermarks and avoiding the retraining procedure. The IQP module uses noise and augmentation operations to subtly embed user-specific information while preserving the high quality of generated images. Consequently, our method achieves seamless integration of watermarking into generative models without compromising image quality. TEAWIB distinguishes itself by enabling the effective management of a substantial user population while maintaining superior image quality over existing integrated watermark embedding methods.

The workflow of TEAWIB is illustrated in Fig. 1. Our framework unfolds through three key steps: (1) The model owner distributes a user-specific watermark and then embeds it into the network as its fingerprint. (2) the model owner modifies pre-trained parameters of the SD decoder. This integration process does not alter the original model parameters but instead enriches them with user-specific watermark information. The integration employs a dynamic blending factor that optimally balances the original pre-trained weights with the new user-specific adjustments. Additionally, noise and augmentation operations are integrated at the pixel level to embed user-specific information subtly, enhancing the robustness of watermarked images against post-processing manipulations. (3) The model user generates images using the fingerprinted decoder, seamlessly embedding invisible watermarks in generated images. This allows the model owner to detect watermarks from potentially unauthorized images.

In summary, our key contributions are:

- We introduce TEAWIB, a novel framework that dynamically and seamlessly integrates watermarking into generative models without compromising the image quality. More importantly, TEAWIB incorporates a “Ready-to-Use” manner, facilitating straightforward integration into existing models without the need for retraining, making it highly accessible and practical in real-world applications.
- To realize TEAWIB, we propose two key modules: Dynamic Watermark Blending (DWB) and Image Quality Preservation (IQP). DWB dynamically adjusts the balance between pre-trained and watermark-specific weights, optimizing watermark robustness without compromising image quality. Concurrently, IQP employs noise and augmentation operations to subtly embed user-specific information, thus maintaining the high-quality appearance of images and ensuring both the effectiveness and invisibility of watermarks.
- Comprehensive experiments on the MS-COCO validation dataset demonstrate the superiority of TEAWIB in both visual quality and attribution accuracy, establishing its position as a state-of-the-art and scalable watermark embedding method.

Related Work

Traditional Watermarking Methods

Traditional watermarking techniques (Al-Haj 2007; Stankovic, Orovic, and Zaric 2010; Sun et al. 2021; Lee, Yoo, and Kalker 2007) focus on embedding messages into the frequency domain of original images by leveraging the Discrete Cosine Transform (DCT) and Discrete Wavelet Transform (DWT). These methods typically involve altering coefficients within specific frequency bands based on carefully designed strategies. However, these traditional methods are post-hoc, making them easily bypassed by malicious users. In contrast, our proposed ad-hoc watermarking method is inherently integrated into the image generation process and cannot be circumvented.

LDM-oriented Watermarking

LDM-oriented watermarking modifies either the initialization of latent vectors or the decoder within LDMs. (Zhang et al. 2024) freezes the decoder and trains the initialization of latent vectors to embed watermarks, preserving perceptual quality. (Fernandez et al. 2023) fine-tunes the decoder of LDM with a user-specific watermark, achieving notable results. However, this method is restricted to a single watermark and requires re-training for any change. (Kim et al. 2024) applies weight modulation to the convolutional layers in the decoder of SD, facilitating the distribution of multiple watermarks. While this method attains satisfactory attribution accuracy, it compromises image quality. Our proposed method addresses this limitation by introducing a watermark-informed blending strategy. This strategy achieves a balance between modified weights and pre-trained weights, resulting in the generation of high-quality images. It also integrates seamlessly into the model through a Ready-to-Use configuration, facilitating easy adoption without the need of complex modifications.

Method

Preliminaries

Our TEAWIB is primarily designed for Stable Diffusion models (SD). For clarity, SD consists of three principal components: the encoder \mathcal{E} , which converts an image I into a latent vector z ; the diffusion model ϵ_θ , built upon the U-Net architecture and augmented by a cross-attention mechanism for textual manipulation; and the decoder \mathcal{D} , which reconstructs an image $\hat{I} = \mathcal{D}(z)$ from the latent vector z . Both the encoder and the decoder are extensively trained on a large dataset to generate realistic images.

Overview

As depicted in Fig. 2, the proposed method is divided into two main stages: (1) model training and (2) model distribution. Modifications are focused solely on the decoder \mathcal{D} , with the diffusion process remaining unchanged, ensuring compatibility across a variety of generative tasks.

In model training, a designated watermark $w \sim \text{Ber}(0.5)^{d_w}$, of length d_w , is selected. This watermark is subsequently transformed into a fingerprint r_w through a

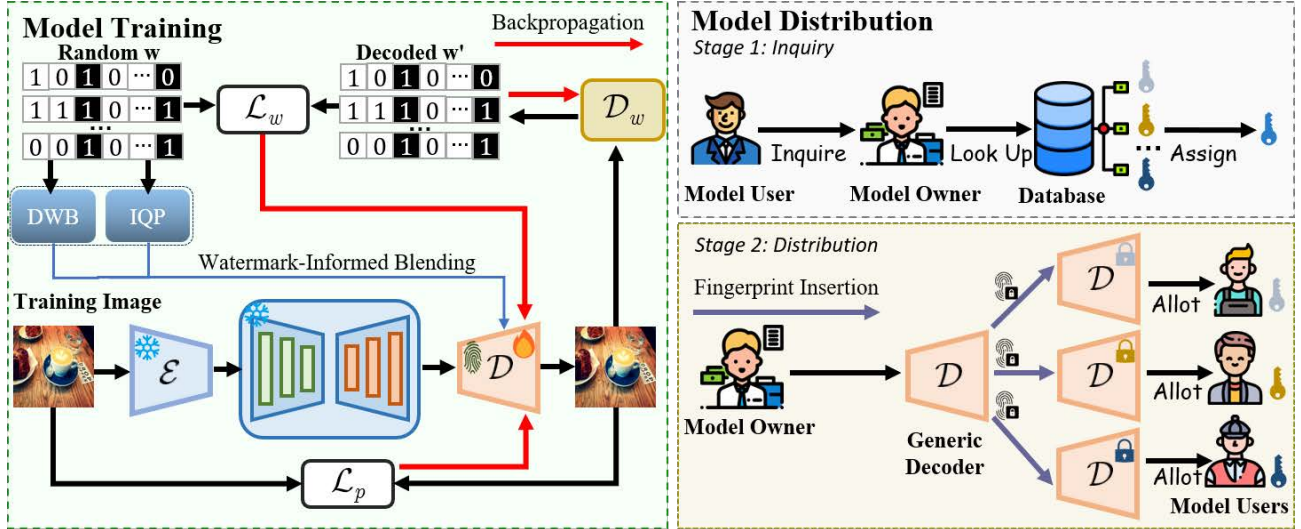


Figure 2: **Overview of TEAWIB.** The workflow is bifurcated into two primary phases: (1) *model training* and (2) *model distribution*. During the training phase, the watermark decoder and the diffusion decoder are concurrently trained using a variety of randomly generated watermarks. The model distribution phase consists of two stages. Stage 1: The model user inquires with the model owner, who performs a lookup operation in the database to assign a distinct watermark to him/her. Stage 2: The model owner embeds the generic decoder with the distinct watermark corresponding to each model user and distributes the watermarked model to the user.

watermark mapping network E_w (built upon two fully connected layers). Subsequently, the fingerprint r_w is leveraged by the proposed watermark-informed blending that embeds the watermark information into model parameters. During the training phase, the decoder \mathcal{D} utilizes both z and r_w as inputs to generate the watermarked image I_w . A watermark decoder \mathcal{D}_w is then employed to extract the watermark message from this image.

The model distribution phase consists of two stages. In the first stage, the model user inquires with the model owner, who will search the database and assign a distinct watermark to this user. In the second stage, model owner fingerprints the trained generic decoder with the user-specific watermark and distributes the fingerprinted model to the corresponding user. It is worth noting that the model has a Ready-to-Use configuration, allowing the owner to easily incorporate the watermark by simply providing it to the generic model.

Watermark-Informed Blending

The proposed watermark-informed blending optimally integrates user-specific watermarks into the model without sacrificing image quality. It comprises two key components: Dynamic Watermark Blending (DWB) and Image Quality Preservation (IQP). The DWB adjusts the blending of original and watermark-specific weights dynamically, ensuring robust watermark embedding with minimal impact on image quality. Simultaneously, the IQP maintains the high quality of images through noise and augmentation operations, enhancing the robustness of the watermark to digital manipulations. Together, these two components ensure that watermarks are effective yet imperceptible, preserving the aesthetic and utility of the generated images.

Dynamic Watermark Blending. Previous methods (Kim et al. 2024) directly modulate the kernel weights and apply them in convolution:

$$y = f_c(\mathbf{W}', x). \quad (1)$$

Here, where y denotes the output feature map, \mathbf{W}' and x denote the fingerprinted weight and input, respectively. f_c represents the convolutional operation.

In Eq. 1, pre-trained weights are modified during fine-tuning. This can lead to issues such as domain shift if the training dataset significantly differs from the original training dataset. Additionally, neglecting the pre-trained weights could potentially result in the loss of valuable information from the initial large-scale training. Pre-trained weights are responsible for generating hyper-realistic images. Additionally, embedding watermark information into the model's parameters is key to implementing ad-hoc watermarking in the Stable Diffusion model. Considering these two factors, we propose the watermark-informed blending that introduces a blending operation into the convolutional process without altering weights of convolutional layers. Inspired by alpha digital image compositing, the final representation of this submodule is formulated as:

$$y_d = \alpha \cdot f_c(\mathbf{W}', x) + (1 - \alpha) \cdot f_c(\mathbf{W}, x), \quad (2)$$

where y_d denotes the blended output feature map, \mathbf{W} represents the pre-trained weights for the convolutional layer, and α is a trainable blending factor. During training, α is optimized based on watermark detection accuracy and perceptual similarity between watermarked images and training images.

Fingerprint Insertion. A fundamental aspect of our approach is the direct insertion of watermark messages into the model

parameters. To integrate them seamlessly, we modulate the convolutional weights of the decoder \mathcal{D} using our fingerprint r_w (the encoded watermark). This technique is inspired by StyleGAN2 (Karras et al. 2020b).

Given a convolutional kernel $\mathbf{W} \in \mathbb{R}^{i \times j \times k}$ at layer l , where i , j , and k denote input channels, output channels, and kernel size, respectively. Initially, a scale factor s and a bias term b are computed. The scale s is obtained by projecting the fingerprint r_w through a Multi-Layer Perceptron (MLP). The bias term b is calculated as $A_l(r_w)$ using an affine transformation layer A_l , where weights of A_l are initialized to zero and the biases are initialized to one. Consequently, $A_l(r_w)$ initially equals a tensor with all ones. This initialization of the bias term provides a stable baseline, ensuring that the scaling of \mathbf{W} is not too extreme at the beginning. The introduction of two learnable terms, s and b , allows the model to better adapt to the data, leading to improved performance.

Subsequently, the channel-wise weight modulation is then executed according to:

$$\mathbf{W}' = \mathbf{W} \cdot (s + b), \quad (3)$$

where \mathbf{W} and \mathbf{W}' denote pre-trained and modulated kernel weights, respectively. We conduct weight modulation for all convolutional layers with the same fingerprint r_w .

Image Quality Preservation. The IQP consists of two operations to preserve image quality and enhance model robustness. Its functionality can be summarized as follows:

$$y_i = aug_t + \lambda_n \cdot \mathcal{N}(0, \sigma^2), \quad (4)$$

where y_i represents the combined result of the two operations: aug_t , which is the augmentation operation, and $\lambda_n \cdot \mathcal{N}(0, \sigma^2)$, which is the noise operation. λ_n is a trainable parameter initialized as 0 to control the magnitude of noise addition.

Noise Operation. To increase the stochastic variation of generated images and refine intricate details, we introduce a randomly generated Gaussian noise $\mathcal{N}(0, \sigma^2)$, which σ represents the standard deviation and sets to 1 following (Karras, Laine, and Aila 2019).

Augmentation Operation. Although the noise operation refines the details, it can degrade robustness against post-processing attacks. To address this issue, we propose an augmentation operation, denoted as aug_t . For layer l , we project the fingerprint r_w through M_l (built upon two fully connected layers), i.e., $aug_t = M_l(r_w)$. This augmentation step operates at the pixel level to embed watermark-related information. Thorough experiments validate that the combination of these two modules can enhance the robustness of the watermark while preserving image quality. The final output y of the Watermark-Informed Blending is formulated as follows:

$$y = y_i + y_d. \quad (5)$$

It incorporates the DWB and IQP to improve both image quality and robustness towards image attacks.

Loss Function

In the training phase, our primary objectives are twofold: 1) accurate message extraction from watermarked images and 2) negligible effect of watermark insertion on the generated images. To achieve the former, we introduce the watermark extraction loss, denoted as \mathcal{L}_w , which also trains a pre-trained watermark extractor \mathcal{D}_w . The message extraction loss between watermark w and extracted message w' is defined as:

$$\mathcal{L}_w = - \sum_{i=1}^{d_w} w_i \cdot \log \epsilon(w'_i) + (1 - w_i) \cdot \log(1 - \sigma(w'_i)), \quad (6)$$

where ϵ represents the Sigmoid function. For the latter objective, we utilize the perceptual loss \mathcal{L}_p . The loss is defined as:

$$\mathcal{L}_p = \lambda_p \cdot \mathcal{L}_v(I_w, I_o) + \lambda_l \cdot \mathcal{L}_l(I_w, I_o), \quad (7)$$

where I_w and I_o are watermarked images and images generated by the original decoder, respectively. \mathcal{L}_v refers to Watson-VGG loss (Czolbe et al. 2020), and \mathcal{L}_l represents LPIPS-loss (Zhang et al. 2018). $\lambda_p = 0.2$, $\lambda_l = 1$ are prescribed coefficients. The total loss \mathcal{L} is given by:

$$\mathcal{L} = \lambda_w \mathcal{L}_w + \mathcal{L}_p, \quad (8)$$

where $\lambda_w = 1$ balances the watermark extraction loss and perceptual loss. The joint optimization of \mathcal{D} and \mathcal{D}_w facilitates the adaptation of \mathcal{D}_w to watermark variations, enhancing its detection accuracy.

Experiments

Experimental Settings

Datasets. The training and evaluation are conducted on the MS-COCO (Lin et al. 2014) dataset of size 256×256 . In line with (Fernandez et al. 2023), 1,000 text prompts from the MS-COCO validation dataset are selected to generate watermarked images.

Diffusion Model Setup. The adopted SD model in TEAWIB uses the same configuration as the repository¹. Specifically, Stable Diffusion 2.0-base is chosen. For text-to-image generation, a guidance scale of 3.0 and 50 diffusion steps are used.

Experimental Setup. Drawing inspiration from the implementation in StyleGAN2-ADA (Karras et al. 2020a), the watermark mapping network E_w comprises two fully connected layers, each with a dimensionality matching that of the fingerprint r_w . For training, the AdamW optimizer (Loshchilov and Hutter 2019) is employed with a learning rate of 10^{-4} . Additionally, the pre-trained watermark extractor from HiDDeN (Zhu et al. 2018) is leveraged.

Evaluation Metrics. To evaluate the quality of generated images, we use PSNR, SSIM (Wang et al. 2004), and LPIPS (Zhang et al. 2018) to measure the similarity between watermarked and original images. Furthermore, we quantify the realism and diversity of watermarked images via FID

¹<https://github.com/Stability-AI/stablediffusion>

Table 1: Comparison of TEAWIB with other merged-in generation methods. Experiments are conducted on images of size 512×512 with 48-bit watermarks. PSNR and SSIM are measured between the generations of the original and watermarked decoders, while FID is computed between original images and watermarked text-generated images. The terms ‘‘Crop’’ and ‘‘Brigh.’’ represent image post-processing steps that crop the image to half of its original size and adjust the brightness by a factor of two. TEAWIB achieves superior performance in terms of generation quality and robustness while being seamlessly integrated into the generation process.

Model	Scalable Watermark	PSNR / SSIM \uparrow	L_∞ \downarrow	LPIPS \downarrow	FID \downarrow	Bit accuracy \uparrow on:		
						None	Crop	Brigh.
Stable Diffusion (Rombach et al. 2022)	–	30.0 / 0.89	–	–	9.294	–	–	–
Stable Signature (Fernandez et al. 2023)	✗	30.0 / 0.89	82.591	0.0330	9.376	0.9918	0.9903	0.9519
WOUAF (Kim et al. 2024)	✓	28.2 / 0.82	130.49	0.0781	18.996	0.9767	0.5912	0.6191
TEAWIB (Ours)	✓	39.2 / 0.98	57.8	0.0047	9.223	0.9919	0.9820	0.9535

(Heusel et al. 2017), and the L_∞ norm is utilized to represent the maximum L-infinity norm between the watermarked and original images. The accuracy of watermark detection, denoted as acc , is measured by Eq. 9.

$$acc = \frac{1}{d_w} \sum_{i=1}^{d_w} \mathbb{1}(w_i = w'_i), \quad (9)$$

where $w' = \mathcal{D}_w(I_w)$ represents the decoded watermark message from the generated image I_w .

Experimental Results

Image quality. Tab. 1 shows the quantitative comparison between our TEAWIB and other merged-in generation methods. Remarkably, TEAWIB demonstrates superior performance across all metrics. The average PSNR has improved significantly from 30.0 dB to approximately 39.2 dB, the SSIM has increased from 0.89 to 0.98, and the lowest FID score is also achieved. Therefore, our TEAWIB can generate images that closely resemble those from the original SD models, in which the presence of watermarks is effectively imperceptible. We also provide the qualitative comparison in Fig. 3. It can be seen that the observed differences between original and watermarked images are negligible, and even when magnified tenfold, the pixel-wise discrepancies remain minimal.

Watermark Detection. To evaluate the watermark detection performance, we use 10 distinct watermarks and generate 1,000 images for each watermark. Experimental results of watermark detection are provided in this subsection, where the detection criterion is defined by the matching bits $M(w, w')$:

$$M(w, w') \geq \tau \text{ where } \tau \in \{0, \dots, d_w\}. \quad (10)$$

Here τ represents the manually selected threshold for detection. Formally, we test the statistical hypothesis H_1 : ‘‘ x was generated by Alice’s model’’ against the null hypothesis H_0 : ‘‘ x was not generated by Alice’s model’’. Under H_0 (i.e. for vanilla images), we assume that bits w'_1, \dots, w'_k are independent and identically distributed (i.i.d.) Bernoulli random variables with parameter 0.5. Consequently, $M(w, w')$ follows a binomial distribution with parameters $(k, 0.5)$. The False Positive Rate (FPR) is the probability that $M(m, m')$

exceeds the threshold τ . It is derived from the Cumulative Distribution Function (CDF) of the binomial distribution, and a closed-form expression can be written using the regularized incomplete beta function $I_x(a, b)$:

$$FPR(\tau) = \mathbb{P}(M > \tau | H_0) = I_{0.5}(\tau + 1, k - \tau), \quad (11)$$

where $x = 0.5$. We select 10 fixed random watermarks and generate 1,000 images for each. We then report the averaged trade-off between the True Positive Rate (TPR) and the FPR, while varying $\tau \in \{0, \dots, 48\}$. The TPR is measured directly, while the FPR is calculated by Eq. 11. The results, displayed in Fig. 4, indicate that our method can achieve a detection accuracy of 99% with a FPR of 10^{-11} if the image is free of any post-processing. However, we also observe that post-processing techniques can lead to a decrease in detection accuracy, which will be discussed later.

Watermark Identification. Watermark identification refers to the scenario where the model owner extracts the watermark w' from suspicious images and identifies the user who generated them. Suppose there are N candidates $w^{(1)}, w^{(2)}, \dots, w^{(N)}$. In the identification task, the global FPR with respect to τ is defined as:

$$FPR(\tau, N) = 1 - (1 - FPR(\tau))^N \approx N \cdot FPR(\tau). \quad (12)$$

For evaluation, we randomly select $N' = 1,000$ watermarks, each of which is used to generate 100 images. For these generated images, we extract watermarks and compute the matching bits with all N watermarks, selecting the user with the highest matching score. An image is predicted to be generated by that user if this score exceeds the threshold τ . We adjust τ in Eq. 12 to fix the FPR at 10^{-6} .

To evaluate the identification accuracy, we increase the total number of watermarks $N (\gg N')$ by adding irrelevant watermarks, thereby testing the robustness of the identification process. The identification results are shown in Fig. 5. It can be seen that the identification accuracy of TEAWIB achieves 99% when $N = 20,000$, validating its capability of watermark identification.

Watermark Robustness. In this paper, the robustness of the watermark is evaluated by adding various post-processing techniques before decoding the watermark. For each transformation, we generate 1,000 images using the prompts from the MS-COCO validation set, each with a



Figure 3: Qualitative comparison of TEAWIB with other ad-hoc watermark generation techniques on the MS-COCO validation set. Notably, our method preserves the high quality of the generated image and invisible watermark embedding.

Table 2: Robustness analysis of TEAWIB and compared methods under various post-processing techniques.

Model	Bit accuracy under various post-processing techniques							
	Bright. 1.5	Sharp 2.0	Sharp 1.5	Text Overlay	Cont. 1.5	Crop 0.1	Sat. 2.0	Sat. 1.5
Stable Signature (Fernandez et al. 2023)	0.9852	0.9829	0.9910	0.9905	0.9808	0.9568	0.9889	0.9910
WOUAF (Kim et al. 2024)	0.8403	0.9758	0.9871	0.9517	0.9588	0.5599	0.8041	0.9607
TEAWIB (Ours)	0.9853	0.9906	0.9914	0.9914	0.9893	0.9295	0.9898	0.9917

randomly selected watermark message. The average bit accuracy is reported in Tab. 1. Compared to WOUAF, our TEAWIB demonstrates superior bit accuracy in the presence of post-processing. While Stable Signature supports only one designated watermark without retraining, making it easier to achieve high bit accuracy, TEAWIB still outperforms it under most post-processing techniques.

Further robustness analysis of TEAWIB and compared methods can be found in Tab. 2, where “Bright. 1.5” refers to increasing the image brightness by $1.5\times$; “Sharp 2.0” and “Sharp 1.5” represent $2\times$ and $1.5\times$ the original image sharpness; “Text Overlay” involves adding texts at random positions in the image; “Cont. 1.5” adjusts the image contrast to $1.5\times$ the original value; “Crop 0.1” reduces the image size to 10% of the original; “Sat. 2.0” and “Sat. 1.5” refer to $2\times$ and $1.5\times$ the original saturation. Even though the watermark decoder is trained jointly during the training phase *without any post-processing augmentation*, our method achieves an average accuracy over 98%, demonstrating its robustness against common image post-processing techniques.

Ablation Study

Watermark-Informed Blending. The proposed WIB is a critical component of our framework, consisting of two main modules: Dynamic Watermark Blending (DWB) and Image Quality Preservation (IQP). DWB focuses on seamlessly integrating watermark-specific weights into the model, while IQP is designed to maintain high image quality through noise operation and augmentation operation.

Therefore, to thoroughly validate its effectiveness, we evaluated four variants to demonstrate the impact of these components on model performance, as detailed in Tab. 3: 1) the baseline model that uses only weight modulation for watermark insertion; 2) Variant 1 that uses only the DWB component, which significantly enhances the model’s ability to produce higher-quality images; 3) Variant 2 excludes the augmentation operation in IQP, demonstrating a significant reduction in model efficacy and highlighting its crucial role in preserving robustness; 4) Variant 3 removes the noise operation in IQP, leading to a noticeable drop in performance and underscoring the necessity of this element for maintaining image quality.

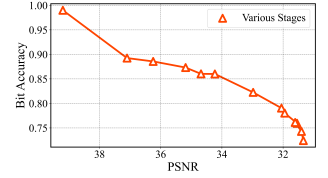
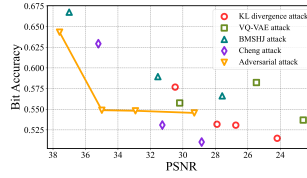
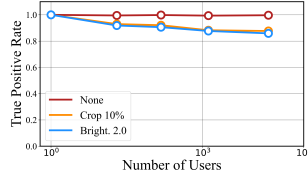
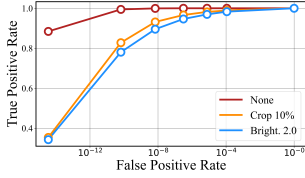


Figure 4: Model detection. Figure 5: Model identification. Figure 6: Image-level attacks. Figure 7: Model purification.

Table 3: Ablation study of TEAWIB. Each variant is evaluated based on four key metrics: PSNR, SSIM, L_∞ , and LPIPS. \uparrow indicates the higher the better, \downarrow indicates the lower the better. *Abbreviation: DWB: Dynamic Watermark Blending; Noise: Noise Operation; Aug: Augmentation Operation; Joint: Jointly training watermark extractor; LPIPS: Use LPIPS Loss. ALL: Use Watermark-Informed Blending across all layers.*

Variant	Training Components						Evaluation Metrics			
	DWB	Noise	Aug	Joint	LPIPS	ALL	PSNR \uparrow	SSIM \uparrow	$L_\infty\downarrow$	LPIPS \downarrow
<i>Reference Results of Baseline Model</i>							28.4	0.86	123.5	0.0614
1	✓					✓	34.8	0.97	64.8	0.0080
2	✓	✓		✓	✓	✓	34.8	0.97	65.5	0.0080
3	✓		✓	✓	✓	✓	38.9	0.98	58.6	0.0051
4	✓	✓	✓	✓		✓	38.9	0.98	59.6	0.0050
5	✓	✓	✓		✓	✓	32.3	0.93	94.7	0.0357
6	✓	✓	✓	✓	✓	✓	31.0	0.91	100.963	0.0345
TEAWIB	✓	✓	✓	✓	✓	✓	39.2	0.98	57.8	0.0047

Training and Network Settings. Effects of other components within the watermark-informed blending method are further investigated. Tab. 3 also outlines various settings of TEAWIB, highlighting the importance of each component in our framework.

Key observations from results include: 1) Variant 4 excludes the LPIPS loss during training, resulting in a decline in performance. This reflects its importance in optimizing the perceptual quality of the output; 2) Variant 5 freezes the watermark decoder throughout the training process. This severely hinders the model’s effectiveness, as evidenced by a marked decrease in performance; 3) Variant 6 omits the watermark-informed blending in the initial and final convolutional layers. This omission greatly compromises the image quality, further demonstrating the importance of these layers in the blending process. Our full model achieves the highest performance across all metrics, highlighting the effectiveness and synergy of the complete design.

Deliberate Attack on Watermarks

This subsection examines the robustness of our method against deliberate attempts to remove watermarks. We consider two types of attacks: image-level attacks, which operate directly on the image, and model-level attacks, which target the decoder \mathcal{D} .

Image Level Attacks. Auto-encoder attack and adversarial attack are common adopted methods to modify output images. The auto-encoder attack refers to passing the generated images through various auto-encoder models. In this paper, we use the VQ-VAE attack (Ballé et al. 2018), KL divergence attack (Rombach et al. 2022), BMSHJ attack (Ballé et al. 2018), and Cheng attack (Cheng et al. 2020).

As shown in Fig. 6, the accuracy of watermark detection gradually decreases as the auto-encoder compression rate increases, eventually approaching a random guess level of around 50%. Although these attacks can reduce watermark detection accuracy, they also severely degrade image quality, making them impractical for the real-world usage.

However, adversarial attack becomes a concern when the watermark extractor \mathcal{D}_w is leaked, attackers can employ adversarial techniques to replace the original watermark with a random one while preserving image quality. These attacks aim to minimize the ℓ_2 distance between a pre-sampled random binary message and the decoded output, effectively substituting the original watermark. As shown in Fig. 6, such attacks can successfully remove watermarks. Therefore, it is necessary for the model owner to ensure the security of the watermark extractor.

Model Level Attacks. In the scenario where an attacker becomes aware of the presence of invisible watermarks, they may attempt to remove them by fine-tuning the diffusion decoder \mathcal{D} . In this context, the attacker’s primary objective is to minimize the reconstruction error between I_w and I_o . The PSNR values between the watermarked and purified images at various stages of fine-tuning are shown in Fig. 7. Our observation indicates that attempts to remove watermarks through model purification result in a degradation of image quality. Therefore, significantly reducing bit accuracy without compromising image quality is challenging, as artifacts tend to emerge during the purification process.

Conclusion

In this paper, we propose a scalable watermarking method dubbed TEAWIB that can effectively perform user attri-

tribution for latent diffusion models via a novel watermark-informed blending and demonstrates the superiority in preserving the high-quality of generated images and achieving near-perfect bit accuracy of watermark extraction. Besides, the robustness of our method is also validated by performing various post-processing techniques on generated images. **Limitation.** Currently, TEAWIB is only applicable to text-to-image generation. Since TEAWIB just slightly modulates the decoder of the Stable Diffusion model, we envision it can also be employed on other generation tasks (*i.e.*, image-to-image, image-to-video, and video-to-video generations). We will expand the applicability of TEAWIB in the future.

References

- Al-Haj, A. 2007. Combined DWT-DCT Digital Image Watermarking. *Journal of Computer Science*, 3(9): 740–746.
- Ballé, J.; Minnen, D.; Singh, S.; Hwang, S. J.; and Johnston, N. 2018. Variational image compression with a scale hyperprior. In *International Conference on Learning Representations*.
- Brundage, M.; Avin, S.; Clark, J.; Toner, H.; Eckersley, P.; Garfinkel, B.; Dafoe, A.; Scharre, P.; Zeitzoff, T.; Filar, B.; Anderson, H.; Roff, H.; Allen, G. C.; Steinhardt, J.; Flynn, C.; hÉigeartaigh, S. Ó.; Beard, S.; Belfield, H.; Farquhar, S.; Lyle, C.; Crootoof, R.; Evans, O.; Page, M.; Bryson, J.; Yampolskiy, R.; and Amodei, D. 2018. The Malicious Use of Artificial Intelligence: Forecasting, Prevention, and Mitigation. *arXiv e-prints*, arXiv:1802.07228.
- Cheng, Z.; Sun, H.; Takeuchi, M.; and Katto, J. 2020. Learned image compression with discretized gaussian mixture likelihoods and attention modules. In *Proceedings of the IEEE/CVF Conference on Computer Vision and Pattern Recognition*, 7939–7948.
- Czolbe, S.; Krause, O.; Cox, I.; and Igel, C. 2020. A loss function for generative neural networks based on watsón’s perceptual model. *Advances in Neural Information Processing Systems*, 33: 2051–2061.
- Fernandez, P.; Couairon, G.; Jégou, H.; Douze, M.; and Furon, T. 2023. The stable signature: Rooting watermarks in latent diffusion models. In *Proceedings of the IEEE/CVF International Conference on Computer Vision*, 22466–22477.
- Fu, K.; Liu, X.; Jia, J.; Zhang, Z.; Peng, Y.; and Wang, J. 2024. RAWIW: RAW Image Watermarking robust to ISP pipeline. *Displays*, 82: 102637.
- Guo, X.; Liu, X.; Ren, Z.; Grosz, S.; Masi, I.; and Liu, X. 2023. Hierarchical fine-grained image forgery detection and localization. In *Proceedings of the IEEE/CVF Conference on Computer Vision and Pattern Recognition*, 3155–3165.
- Heusel, M.; Ramsauer, H.; Unterthiner, T.; Nessler, B.; and Hochreiter, S. 2017. Gans trained by a two time-scale update rule converge to a local nash equilibrium. *Advances in neural information processing systems*, 30.
- Karras, T.; Aittala, M.; Hellsten, J.; Laine, S.; Lehtinen, J.; and Aila, T. 2020a. Training generative adversarial networks with limited data. *Advances in neural information processing systems*, 33: 12104–12114.
- Karras, T.; Laine, S.; and Aila, T. 2019. A style-based generator architecture for generative adversarial networks. In *Proceedings of the IEEE/CVF conference on computer vision and pattern recognition*, 4401–4410.
- Karras, T.; Laine, S.; Aittala, M.; Hellsten, J.; Lehtinen, J.; and Aila, T. 2020b. Analyzing and improving the image quality of stylegan. In *Proceedings of the IEEE/CVF conference on computer vision and pattern recognition*, 8110–8119.
- Kim, C.; Min, K.; Patel, M.; Cheng, S.; and Yang, Y. 2024. WOUAF: Weight Modulation for User Attribution and Fingerprinting in Text-to-Image Diffusion Models. In *Proceedings of the IEEE/CVF Conference on Computer Vision and Pattern Recognition (CVPR)*, arXiv:2306.04744.
- Kishore, V.; Chen, X.; Wang, Y.; Li, B.; and Weinberger, K. Q. 2022. Fixed Neural Network Steganography: Train the images, not the network. In *International Conference on Learning Representations*.
- Lee, S.; Yoo, C. D.; and Kalker, T. 2007. Reversible Image Watermarking Based on Integer-to-Integer Wavelet Transform. *IEEE Transactions on Information Forensics and Security*, 2(3): 321–330.
- Lin, T.-Y.; Maire, M.; Belongie, S.; Hays, J.; Perona, P.; Ramanan, D.; Dollár, P.; and Zitnick, C. L. 2014. Microsoft coco: Common objects in context. In *Computer Vision—ECCV 2014: 13th European Conference, Zurich, Switzerland, September 6–12, 2014, Proceedings, Part V 13*, 740–755. Springer.
- Liu, X.; Liu, Y.; Chen, J.; and Liu, X. 2022. PSCC-Net: Progressive spatio-channel correlation network for image manipulation detection and localization. *IEEE Transactions on Circuits and Systems for Video Technology*, 32(11): 7505–7517.
- Loshchilov, I.; and Hutter, F. 2019. Decoupled Weight Decay Regularization. In *International Conference on Learning Representations*.
- Luo, X.; Zhan, R.; Chang, H.; Yang, F.; and Milanfar, P. 2020. Distortion agnostic deep watermarking. In *Proceedings of the IEEE/CVF conference on computer vision and pattern recognition*, 13548–13557.
- Nichol, A.; Dhariwal, P.; Ramesh, A.; Shyam, P.; Mishkin, P.; McGrew, B.; Sutskever, I.; and Chen, M. 2021. GLIDE: Towards Photorealistic Image Generation and Editing with Text-Guided Diffusion Models. In *International Conference on Machine Learning*.
- Ramesh, A.; Dhariwal, P.; Nichol, A.; Chu, C.; and Chen, M. 2022. Hierarchical Text-Conditional Image Generation with CLIP Latents. *arXiv e-prints*, arXiv:2204.06125.
- Rombach, R.; Blattmann, A.; Lorenz, D.; Esser, P.; and Ommer, B. 2022. High-resolution image synthesis with latent diffusion models. In *Proceedings of the IEEE/CVF conference on computer vision and pattern recognition*, 10684–10695.
- Saharia, C.; Chan, W.; Saxena, S.; Li, L.; Whang, J.; Denton, E. L.; Ghasemipour, K.; Gontijo Lopes, R.; Karagol Ayan,

- B.; Salimans, T.; et al. 2022. Photorealistic text-to-image diffusion models with deep language understanding. *Advances in neural information processing systems*, 35: 36479–36494.
- Stankovic, S.; Orovic, I.; and Zaric, N. 2010. An Application of Multidimensional Time-Frequency Analysis as a Base for the Unified Watermarking Approach. *IEEE Transactions on Image Processing*, 19(3): 736–745.
- Sun, W.; Zhou, J.; Li, Y.; Cheung, M.; and She, J. 2021. Robust High-Capacity Watermarking Over Online Social Network Shared Images. *IEEE Transactions on Circuits and Systems for Video Technology*, 31(3): 1208–1221.
- Wang, Z.; Bovik, A.; Sheikh, H.; and Simoncelli, E. 2004. Image quality assessment: from error visibility to structural similarity. *IEEE Transactions on Image Processing*, 13(4): 600–612.
- Wu, G.; Wu, W.; Liu, X.; Xu, K.; Wan, T.; and Wang, W. 2023. Cheap-fake Detection with LLM using Prompt Engineering. In *2023 IEEE International Conference on Multimedia and Expo Workshops (ICMEW)*, 105–109. IEEE.
- Yang, Y.; Liu, Z.; Jia, J.; Gao, Z.; Li, Y.; Sun, W.; Liu, X.; and Zhai, G. 2024. DiffStega: Towards Universal Training-Free Coverless Image Steganography with Diffusion Models. arXiv:2407.10459.
- Zhang, L.; Liu, X.; Viros Martin, A.; Xiong Bearfield, C.; Brun, Y.; and Guan, H. 2024. Robust Image Watermarking using Stable Diffusion. *arXiv e-prints*, arXiv:2401.04247.
- Zhang, R.; Isola, P.; Efros, A. A.; Shechtman, E.; and Wang, O. 2018. The Unreasonable Effectiveness of Deep Features as a Perceptual Metric. *arXiv e-prints*, arXiv:1801.03924.
- Zhu, J.; Kaplan, R.; Johnson, J.; and Fei-Fei, L. 2018. HiD-DeN: Hiding Data With Deep Networks. In *European Conference on Computer Vision*.